Improving Optical Confinement in Nanostructures via External Mode Coupling

Q. H. Song and H. Cao

Department of Applied Physics, Yale University, New Haven, Connecticut, 06520, USA

(Received 1 January 2010; revised manuscript received 28 June 2010; published 26 July 2010)

We demonstrate the formation of long-lived resonances via external coupling in open nanostructures. In the examples of three dielectric nanorods or strips, external coupling of modes is induced by tuning of the rod spacing and increases the lifetime over an order of magnitude. Such an enhancement results from the destructive interference of fields that minimizes light leakage. Our results illustrate an effective way of storing light in nanostructures, and have potential applications to nanoscale photonic devices.

DOI: 10.1103/PhysRevLett.105.053902 PACS numbers: 42.79.Gn, 05.45.Mt, 42.25.−p, 81.07.Gf

Strong confinement of light in a nanometer volume can greatly enhance light-matter interactions. It is essential to the developments of nanophotonic devices with superior performances, such as nanolasers, photodetectors, nonlinear optical switches and frequency converters [1–3]. The parameter that characterizes the degree of light confinement is the quality (Q) factor, which is proportional to the confinement time in units of the optical period [1]. Although the photonic crystal defect modes have extremely high Q and ultrasmall mode volumes, the overall sizes of periodic structures are at least several microns [4]. The metallic nanocavities can have much smaller overall size, but the dissipative loss of metal dramatically reduces the Q factor [5–7]. Another type of nanostructures that has been extensively studied is semiconductor nanowires [3]. The large refractive index difference between the semiconductor material and the surrounding dielectric environment enables photonic confinement in the nanowire. Lasing has been realized in the axial Fabry-Perot waveguide modes of well-faceted nanowires with diameters 100–500 nm [8]. However, significant optical loss at the end facets prevents lasing in the nanowires of length shorter than 1 μm because the quality factor drops quickly with decreasing wire length. How can we keep the Q factor relatively high while reducing the length to submicron? With a rapid progress in the growth and fabrication of nanorod arrays [9], collective resonance in a few nanorods becomes a promising way.

Proximity resonances are well known in a broad physical context, e.g., scattering of sound waves from small bubbles in liquids, light emission from nearby dipoles that leads to Dicke superradiance and subradiance, electrons confined in multiple quantum wells, and coupling of microcavities that form photonic molecules [10–13]. When two nanorods are placed within one wavelength, the electromagnetic resonances of individual rods can be coupled via evanescent field and form new resonances which are called proximity resonances. The Q factor of a proximity resonance may be significantly higher than that of the resonance of a single constituent rod (when two rods are far apart), but it is usually lower than that of the rod with the same length and a cross section equal to the total area of the composite system of two rods [14]. However, this is no longer true for three nanorods, as to be shown in this Letter, thanks to the external coupling of proximity resonances.

In open or dissipative systems, resonances may couple internally and/or externally. In the former each resonance is coupled individually to the continuum, while in the latter the resonances couple through the continuum. If the coupling is strong, the resonant frequencies anticross and the wave functions exchange. In the case of weak coupling, the resonant frequencies cross, and there is a slight mixing of wave functions but no exchange of ''identity.'' Strong external coupling can form long-lived states, as shown by Wiersig in optical microcavities [15]. Surprisingly, weak external coupling also leads to a great enhancement of lifetime, as we will demonstrate with three nanorods here. Our results illustrate that external coupling provides an effective mechanism for controlling light leakage from nanostructures.

Coupling of two resonances can be understood in terms of a 2×2 Hamiltonian matrix [15]

$$H = \begin{pmatrix} E_1 & V \\ W & E_2 \end{pmatrix}. \tag{1}$$

E_1 and E_2 are complex energies of the uncoupled system, W and V are coupling constants. The eigenstates of the coupled system can be obtained by diagonalization of the matrix. The eigenvalues are

$$E_{\pm}(\Delta) = \frac{E_1 + E_2}{2} \pm \sqrt{\frac{(E_1 - E_2)^2}{4} + VW}. \tag{2}$$

The imaginary parts of $E_{\pm}$ are negative, and the amplitudes $|\mathrm{Im}[E_{\pm}]|$ are inversely proportional to the lifetimes of the two eigenstates. Their quality factors $Q_{\pm} = \mathrm{Re}[E_{\pm}]/2|\mathrm{Im}[E_{\pm}]|$. We take $\mathrm{Re}[E_2] - \mathrm{Re}[E_1] = \Delta$ as a variable, and assume $\mathrm{Im}[E_1]$, $\mathrm{Im}[E_2]$, V and W are independent of Δ. In the case of internal coupling, $V = W^*$, and VW is a real positive number. When $VW > |\mathrm{Im}[E_2] - \mathrm{Im}[E_1]|/2$, the coupling is strong enough to cause an avoided crossing in the real parts of $E_{\pm}$ at $\Delta = 0$. For weak coupling $VW < |\mathrm{Im}[E_2] - \mathrm{Im}[E_1]|/2$, the real parts

of $E_\pm$ cross, as shown in Fig. 1(a). The longer-lived state (with smaller $|\mathrm{Im}[E]|$) has an increase in $|\mathrm{Im}[E]|$ (a decrease in $\mathrm{Im}[E]$ as it has a negative value), thus its Q is reduced [Fig. 1(b)]. Meanwhile the Q of the shorter-lived state is increased via coupling to the longer-lived one. Hence, the internal coupling cannot enhance the Q of the longer-lived state. However, in the case of external coupling where $V \neq W^*$ and VW is a complex number, the resonances of an open system are coupled via the continuum and unexpected effects appear. It has been shown that strong external coupling can produce long-lived, scarlike modes in open microcavities [15]. Here we explore the weak external coupling. As shown in Fig. 1(a), the real parts of $E_\pm$ cross around $\Delta = 0$, similar to the case of weak internal coupling. However, the variation of the imaginary parts with Δ in the weak external coupling is very different from that of internal coupling. The Q value of the longer-lived state can be significantly enhanced near $\Delta = 0$, while that of the shorter-lived one is reduced. Different results are obtained for $VW = 0.0001 + i0.000225$ and $-0.0001 + i0.000225$, indicating the Q enhancement depends on not only the amplitude but also the phase of coupling constants. Our numerical calculation with various values of VW shows that large Q enhancement usually happens when VW is far from a real positive number. This means the external coupling must be dominant over the internal coupling ($V = W*$ and VW is a real positive number). Such phenomenon bears resemblance to the resonance trapping that has been studied in atomic, molecular and mesoscopic physics [16,17].

We apply the above general theory to three dielectric nanorods. We first simulate a simplified two-dimensional (2D) structure, then move to the realistic 3D structure. The 2D structure, drawn schematically in the inset of Fig. 2(b), has three identical dielectric nanostrips in air. Each strip is 400 nm long and 50 nm wide. The spacing between adjacent strips is d. The refractive index of the dielectric strips is 3.5. In the wavelength range of simulation ($500\ \mathrm{nm} \leq \lambda \leq 1200\ \mathrm{nm}$), a single strip supports only the fundamental guided mode for TE polarization [electric field perpendicular to the xz plane].

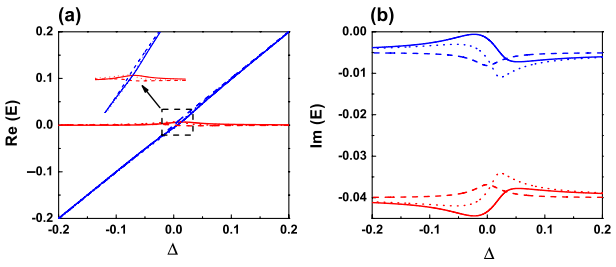

FIG. 1 (color online). Real (a) and imaginary (b) parts of eigenenergies $E_\pm$ of the Hamiltonian matrix (1) as a function of Δ. $E_1 = -i0.04$, and $E_2 = \Delta - i0.005$. Dashed curves represent a weak internal coupling with $VW = 0.0001$, the solid and dot curves are weak external couplings with $VW = -0.0001 + i0.000225$ and $0.0001 + i0.000225$, respectively.

We calculate the TE modes in the three strips using the finite element method [18]. Figure 2 shows two resonant modes cross in wavelength at $d = 33$ nm. Near the crossing, one mode (labeled A) has a dramatic increase of Q, while the other (mode B) has a shallow dip in Q. Such phenomena indicate these two resonances of the three-strip system are coupled at their frequency crossing. Their coupling can be described by the 2×2 Hamiltonian matrix in Eq. (1), because other modes are detuned and their coupling to these two modes can be neglected. The behaviors of the two coupled modes agree qualitatively to the results of weak external coupling in Fig. 1. The electric field distributions of modes A and B, plotted in Fig. 3 for $d = 10$ nm, 31 nm and 80 nm, show that there is no exchange of wave functions when they pass through the crossing point, confirming they are weakly coupled. Nevertheless, the weak coupling of modes A and B results in a mixing of their wave functions, as evident from the slight modifications of the field patterns in Figs. 3(c) and 3(d). For mode A, field intensities near the ends of two side strips are reduced via destructive interference. Light leakage from these locations are suppressed, leading to an increase of Q. For mode B, the constructive interference enhances light leakage from the strip ends, thus its Q is decreased. The maximal Q of mode A is about 160, which is over 30 times higher than that of the mode in a single strip. For comparison, we also calculate the Q factor of 1 strip whose width is equal to the total width of the composite system ($3 \times 50 + 2 \times 30 = 210$ nm). Its value is 55, about 3 times lower than the maximal Q of the three separate strips.

Although weak coupling has been widely studied in open systems such as microcavities, large Q enhancement has not been reported before [19–21]. One significant difference between our system and the previously studied ones is that the Q values of long-lived resonances are much larger in the latter. Higher Q means less leakage of light to the continuum. Hence, the continuum plays a minor role in mode coupling. The internal coupling dominates, which increases the Q of the shorter-lived mode instead of the longer-lived one (dashed line in Fig. 1). In our nanostructures, even the longer-lived modes have relatively low Q. Hence, the external coupling becomes dominant, and pro-

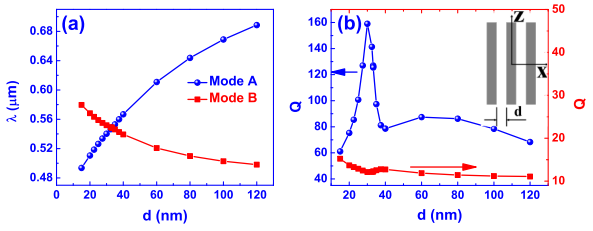

FIG. 2 (color online). Calculated wavelengths λ (a) and Q factors (b) of mode A and B in three nanostrips as a function of the spacing of adjacent strips d. Inset: Schematic diagram of three dielectric nanostrips. Each strip is 400 nm long and 50 nm wide, its refractive index $n = 3.5$.

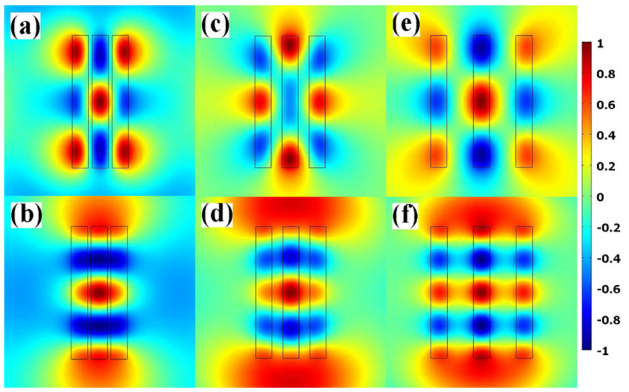

FIG. 3 (color online). Calculated electric field distributions for modes A (top row) and B (bottom row) of three nanostrips with spacing $d = 10$ nm [(a),(b)], 31 nm [(c),(d)], and 80 nm [(e),(f)]. Each field pattern is normalized so that the maximal field amplitude is equal to unity.

vides an effective way of enhancing Q of the longer-lived resonances.

To further increase Q, we coat the strip ends with 100 nm silver as drawn schematically in the inset of Fig. 4(b). The dielectric function of silver is calculated with the Drude model [22]: $\epsilon(\omega) = \epsilon_\infty - \omega_p^2/\omega(\omega + i\Gamma)$, where $\epsilon_\infty = 3.92$, $\omega_p = 1.33 \times 10^{16}$ Hz, and $\Gamma = 2.73 \times 10^{13}$ Hz. Despite absorption, the silver coating enhances light reflection at the ends of dielectric strips. For a single dielectric strip, Q is increased from 5 to 42 with silver coating, but it is still low.

Next we induce strong external coupling of resonances in three metal-coated nanostrips to push Q to a couple of thousands. Figure 4 plots λ and Q of two modes as a function of the spacing d of adjacent strips. The modes experience an anticrossing in λ at $d = 25$ nm, and they exchange the field patterns while passing through the anticrossing (Fig. 5). These results indicate the two modes are strongly coupled. The reason the coupling becomes strong is that in the metal-coated nanostrips the difference in the leakage rates ($\mathrm{Im}[E_{1,2}]$) of the modes is reduced. Close to the anticrossing, the Q of mode 1 rises sharply to about 1800, while that of mode 2 gradually drops. Such behavior reveals the coupling is predominantly external.

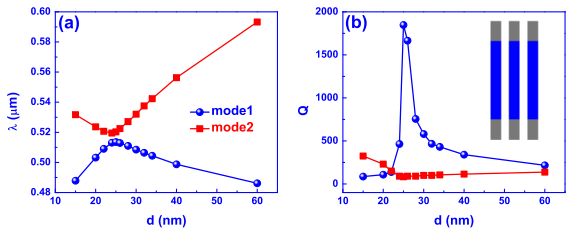

FIG. 4 (color online). Calculated wavelength λ (a) and Q factor (b) of two coupled modes (1, 2) in three dielectric nanostrips with silver coating as a function of the spacing of adjacent strips d. Inset of (b): a schematic diagram of three dielectric strips with 100 nm silver coating on each end.

Around the anticrossing, there is a strong mixing of the field patterns. One hybrid mode [Fig. 5(c)] has reduced field intensities near the metal or dielectric interfaces of two side strips, where most light leakage occurs. This is attributed to the destructive interference of two mode patterns, that increases the Q over an order of magnitude. The other hybrid mode has enhanced field intensities at the ends of two side strips as a result of constructive interference of two field patterns. The increased light leakage reduces the Q. The maximal Q of three metal-coated nanostrips is about 40 times higher than that of a single one. We also compare it to the Q of a single metal-coated strip with a width equal to the total width of the composite system. The latter is 240, which is over 7 times lower than the former.

We emphasize that the drastic Q enhancement cannot be simply explained by the optical confinement induced by metal coating, which is a well-known effect and has been applied to nanocavities [5]. When the three nanostrips are far apart, the resonances in individual strips are uncoupled and the Q is merely 42 even with the enhanced reflection from the strip ends by the metal coating. The increase of Q to 1800 at $d = 25$ nm is attributed to the strong coupling of modes. Namely, the hybridization of field patterns dramatically reduces light leakage via the interference effect. Moreover, surface plasmon resonances are not involved in the modes studied here, unlike some recent works of metallic cavities [6,7,23].

Although the 2D simulation results illustrate the effects of mode couplings on Q factors, the realistic structures are three dimensional. Next we present the 3D simulation results. The structure is schematically drawn in the inset of Fig. 6(a), three nanorods of circular cross section ($n = 3.5$) standing on a silica substrate ($n = 1.45$). The nanorods are 800 nm in height and 90 nm in radius. We increase the rod size in order to scale the resonant frequencies to near infrared, where the refractive indices of many common semiconductors are close to 3.5. Again we find two

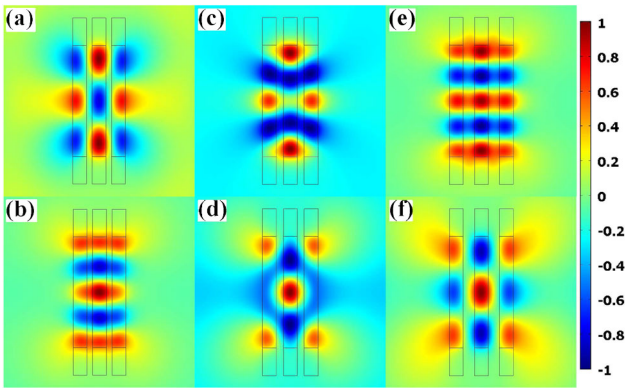

FIG. 5 (color online). Calculated electric field distributions of two coupled modes in three silver-coated dielectric nanostrips at $d = 20$ nm [(a),(b)], 25 nm [(c),(d)], and 40 nm [(e),(f)]. Mode 1 (a), (c), (e) and mode 2 (b), (d), (f) exchange their field patterns after the avoided crossing in wavelength [Fig. 4(a)].

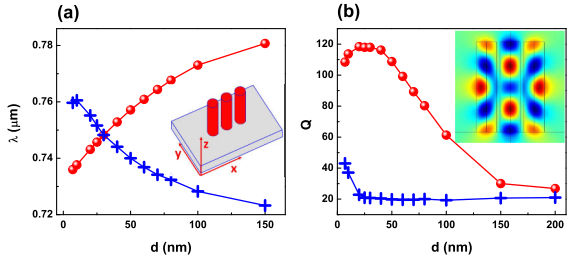

FIG. 6 (color online). Inset of (a) is a schematic diagram of three nanorods ($n = 3.5$) standing on top of a silica substrate ($n = 1.45$). The nanorods, surrounded by air ($n = 1$), are 800 nm in height and parallel to the z axis. Their cross sections in the xy plane are circles of radius 90 nm. The wavelengths and Q values of two resonances as a function of the nearest surface-to-surface distance of adjacent rods d are plotted in (a) and (b). Inset of (b) is the spatial distribution of electric field in the vertical cross section through the axes of all three rods (xz plane) for the higher-Q mode at $d = 30$ nm.

modes cross in wavelength at the inter-rod distance $d \sim 30$ nm [Fig. 6(a)]. Near the crossing, the Q of one mode increases a lot, while the other one decreases slightly [Fig. 6(b)]. Such behavior is similar to that in the 2D case of weak external coupling (Fig. 2). There is no exchange of field patterns when the two modes cross in wavelength, confirming their coupling is weak. Nevertheless, the coupling causes slight mixing of two mode patterns, as can be seen from the small distortion of the spatial field distribution of the higher-Q mode [inset of Fig. 6(b)]. These results confirm that the mechanism of Q enhancement via mode coupling works well for the realistic nanorod structures, which can be fabricated by the well-developed nanofabrication techniques.

For the results presented above, the refractive indices n are assumed constant. To check the effect of material dispersion, we repeat the calculation using $n(\lambda)$ of specific semiconductors, e.g., AlGaAs. Similar results are obtained. Since two modes can couple only when they are close in frequency, they have nearly identical values of refractive index. The spectral range of mode coupling is relatively narrow and the variation of n with λ is negligible for most materials. When the nanorods or strips have lower n, the Q enhancement becomes weaker, but remains significant in a relatively broad range of n. For example, Q of three nanostrips with $n = 2.5$ can be an order of magnitude higher than that of a single trip. Similarly, if the nanorods or strips are buried in a dielectric material of $n_s > 1$, Q enhancement is also reduced compared to that in air. However, if the nanorods or strips are covered with a thin layer of dielectric material (n_s) instead [5], the decrease in the magnitude of Q enhancement is much smaller.

Finally we compute the effective mode volume V_{eff} in the three-nanorod structure, and compare to the values of microcavities. For the higher-Q mode at the crossing [Fig. 6], $V_{\text{eff}} = 1.06(\lambda/n)^3$. This value is smaller than the mode volumes in most microcavities [1]. The only one that has comparable V_{eff} is the photonic crystal defect cavity. However, the overall size of such structure is much larger, because strong light confinement is achieved by Bragg scattering over many periods of unit cells. The tiny footprint of our structure is essential to the application in nanophotonic circuits. Because our structure is submicron in all dimensions, the maximal Q is not high compared to those of the microcavities whose sizes are at least a few micron [1]. Nevertheless, the Q of three nanorods is considerably higher than those of nanocavities in which lasing has been realized recently [5,6]. More importantly, we have demonstrated an effective scheme of improving Q dramatically without a significant increase of the overall structure size. Considering the fact that resonances in the nanocavities have low Q and thus large coupling through the continuum, we believe our scheme based on external coupling is general and applicable to a wide range of nanostructures. The efficient confinement of light in nanostructures is crucial to the developments of nanoscale optical devices with high performance.

The authors thank Jan Wiersig for discussions. This work is funded by NIST Grant No. 70NANB6H6162 and NSF Grant No. DMR-0808937.

[1] K. J. Vahala, Nature (London) **424**, 839 (2003).
[2] T. Tanabe, M. Notomi, S. Mitsugi, A. Shinya, and E. Kuramochi, Opt. Lett. **30**, 2575 (2005).
[3] R. X. Yan, D. Gargas, and P. D. Yang, Nat. Photon. **3**, 569 (2009).
[4] S. Noda, Science **314**, 260 (2006).
[5] M. T. Hill *et al.*, Nat. Photon. **1**, 589 (2007).
[6] M. A. Noginov *et al.*, Nature (London) **460**, 1110 (2009).
[7] R. F. Oulton *et al.*, Nature (London) **461**, 629 (2009).
[8] M. H. Huang *et al.*, Science **292**, 1897 (2001).
[9] Y. N. Xia *et al.*, Adv. Mater. **15**, 353 (2003).
[10] E. J. Heller, Phys. Rev. Lett. **77**, 4122 (1996).
[11] M. Bayer *et al.*, Phys. Rev. Lett. **81**, 2582 (1998).
[12] S. Ishii and T. Baba, Appl. Phys. Lett. **87**, 181102 (2005).
[13] S. Boriskina, Opt. Lett. **31**, 338 (2006).
[14] This statement is based on our numerical simulation results of 2 nanorods, each supports only the fundamental waveguide mode.
[15] J. Wiersig, Phys. Rev. Lett. **97**, 253901 (2006).
[16] E. Persson *et al.*, Phys. Rev. Lett. **85**, 2478 (2000).
[17] M. Desouster-Lecomte and V. Jacquest, J. Phys. B **28**, 3225 (1995).
[18] Commercial program Comsol Multiphysics 3.5a.
[19] J. Wiersig and M. Hentschel, Phys. Rev. A **73**, 031802 (2006).
[20] S. B. Lee *et al.*, Phys. Rev. A **80**, 011802(R) (2009).
[21] S. B. Lee *et al.*, Phys. Rev. Lett. **103**, 134101 (2009).
[22] P. Drude, Ann. Phys. (Leipzig) **306**, 566 (1900).
[23] B. Min *et al.*, Nature (London) **457**, 455 (2009).